High-quality Bi2Te3 thin films grown on mica substrates for potential optoelectronic applications

Article *in* Applied Physics Letters · July 2013

DOI: 10.1063/1.4813903

AIP | Applied Physics Letters

High-quality Bi2Te3 thin films grown on mica substrates for potential optoelectronic applications

K. Wang, Yanwen Liu, Weiyi Wang, N. Meyer, L. H. Bao et al.

Citation: Appl. Phys. Lett. **103**, 031605 (2013); doi: 10.1063/1.4813903
View online: http://dx.doi.org/10.1063/1.4813903
View Table of Contents: http://apl.aip.org/resource/1/APPLAB/v103/i3
Published by the AIP Publishing LLC.

High-quality Bi_2Te_3 thin films grown on mica substrates for potential optoelectronic applications

K. Wang,[1,2] Yanwen Liu,[1] Weiyi Wang,[1] N. Meyer,[2] L. H. Bao,[1,2] L. He,[3] M. R. Lang,[3] Z. G. Chen,[4] X. Y. Che,[2] K. Post,[5] J. Zou,[4,6] D. N. Basov,[5] K. L. Wang,[3] and Faxian Xiu[1,a)]
[1]*State Key Laboratory of Surface Physics and Department of Physics, Fudan University, Shanghai 200433, China*
[2]*Department of Electrical and Computer Engineering, Iowa State University, Ames, Iowa 50011, USA*
[3]*Device Research Laboratory, Department of Electrical Engineering, University of California, Los Angeles, California 90095, USA*
[4]*Materials Engineering, The University of Queensland, Brisbane QLD 4072, Australia*
[5]*Department of Physics, University of California, San Diego, California 92093, USA*
[6]*Center for Microscopy and Microanalysis, The University of Queensland, Brisbane QLD 4072, Australia*

(Received 15 April 2013; accepted 26 June 2013; published online 17 July 2013)

We report high-quality topological insulator Bi_2Te_3 thin films grown on muscovite mica substrates by molecular beam epitaxy. The topographic and structural analysis revealed that the Bi_2Te_3 thin films exhibited atomically smooth terraces over a large area and a high crystalline quality. Both weak antilocalization effect and quantum oscillations were observed in the magnetotransport of the relatively thin samples. A phase coherence length of 277 nm for a 6 nm thin film and a high surface mobility of 0.58 $m^2\ V^{-1}\ s^{-1}$ for a 4 nm thin film were achieved. These results confirm that the thin films grown on mica are of high quality. © *2013 AIP Publishing LLC*.
[http://dx.doi.org/10.1063/1.4813903]

Three-dimensional topological insulators (3DTIs) exhibit a feature of gapless surface states inside the bulk bandgap, promising potential applications in spintronics, quantum computation, and thermoelectrics.[1] To probe the exotic phenomena arising from the topologically protected surface states in 3DTI, the exploitation of high quality materials is of crucial importance. In practice, because of the crystal imperfections generated during growth, the carrier density of bulk outnumbers the surface state, thus, masking the signature of the surface transport.[2] For achieving large-area TI thin films and heterostructures, molecular beam epitaxy (MBE) has demonstrated advantages in precisely controlling the growth rate and obtaining low-defect-density epilayers. However, owing to the lattice mismatch between substrates and thin films, amorphous layers often develop along the interfaces. Additionally, due to the spirals growth behavior, the steps and voids are produced among the terraces on the surfaces of the thin films, giving rise to a small effective surface conductance.[3–6]

One promising approach to improve the crystalline quality is to grow thin films on weakly interacting substrates via van der Waals epitaxy (vdWE), which facilitates the growth of a defect-free epilayer with its own lattice parameters even from the first layer.[7] Muscovite mica with a stoichiometry of $KAl_3Si_3O_{10}(OH)_2$ is a well-known substrate that favors the vdWE growth of semiconductors, metal thin films, and well-oriented nanowire arrays.[8] Its perfect electrical and thermal insulation, high transparency in ultrathin thickness, and flexibility make it an ideal substrate for TI thin film growth and the investigation of the corresponding electrical and optical properties. As a typical 3DTI material, Bi_2Te_3 has a rhombohedral crystal structure consisting of quintuple layers (QLs) stacked along [111] direction.[9] Here, we performed the growth of high-quality Bi_2Te_3 thin films on mica substrates by MBE. The achieved Bi_2Te_3 thin films exhibit ultra-smooth surfaces with large-area terraces as revealed by atomic force microscopy (AFM). Both the weak antilocalization (WAL) effect and quantum oscillations were observed in the ultrathin thin films by the magnetotransport transport measurements. The high quality of the thin films on mica substrates was confirmed by the relatively long phase coherence length and the high surface mobility of electrons.

Bi_2Te_3 thin films were grown on freshly cleaved mica in a Perkin-Elmer 430 MBE system with a base pressure of $\sim 3 \times 10^{-10}$ Torr. Reflection high energy electron diffraction (RHEED) was used to monitor the quality of the thin film during growth. The topography of thin films was examined by AFM in a tapping mode, and the thickness was reliably determined by scanning a scratch deliberately made on as-grown thin films. The growth rate of the Bi_2Te_3 was maintained at ~0.5 QL/min. Further structural analyses were carried out on a Siemens D-500 X-ray diffractometer (XRD) and a Raman spectrometer (Renishaw) with a 514.5 nm laser. The optical properties of the Bi_2Te_3 thin films on mica were examined by UV-Vis-IR spectrophotometer (Cary 5000) at room temperature. Magnetotransport measurements were performed on Hall bar structures in a Physical Property Measurement System (PPMS). The dimension of the Hall bars was defined by a physical mask by the reactive ion etching. The magnetic field was applied perpendicularly to the plane of Hall bar devices. Both the longitudinal sheet resistance (R_s) and Hall resistance (R_{yx}) were simultaneously recorded by sweeping the magnetic field between −9 T and +9 T at programmed temperatures.

a)Author to whom correspondence should be addressed. Electronic mail: Faxian@fudan.edu.cn. Tel.: 011-86-21-51630277.

Representative topographic AFM images of 4 and 10 QLs Bi_2Te_3 thin films were shown in Figs. 1(a) and 1(b), respectively, revealing the ultra-smooth surfaces with large-area terraces. Quantitatively, the overall root-mean-square roughness of 4 and 10 QLs thin films over a large area ($5 \times 5\,\mu m^2$) was determined to be 0.103 and 0.283 nm, respectively. As plotted in Fig. 1(c), the height profile along the dashed line drawn in Fig. 1(b) shows the thickness of 1 QL in Bi_2Te_3, suggesting a layer-by-layer growth mode. The terrace with an area up to $\sim 3\,\mu m^2$ observed here is large compared to the reported MBE-grown TI thin films.[10] Previously, the surfaces of Bi_2Te_3 or Bi_2Se_3 thin film often comprised some domains of pyramidal-shape terraces or so-called triangular spirals; consequently, depending on the thickness of the thin films, a large number of valleys/voids with varied depths/sizes could exist in between two adjacent domains.[5,11] In sharp contrast, the terraces of our Bi_2Te_3 thin films on mica present nearly full coverage of the entire surface over a large area with only one or two QLs variation in thickness. The absence of spirals on the terraces, together with the shape of the terrace, suggests a favorable growth dynamics accounting for the high crystalline quality of TI on mica.[12] To acquire strong signals, a relatively thick Bi_2Te_3 thin film of 45 QLs was used for obtaining Raman spectra and XRD patterns. Figure 1(d) shows a typical Raman spectrum with two characteristic peaks centering at 103.0 cm^{-1} and 134.9 cm^{-1}, respectively. These two vibration modes can be identified as in-plane vibration E_g^2 and out-of-plane vibration A_{1g}^2, which is in excellent agreement with the reported bulk Bi_2Te_3 and MBE-grown Bi_2Te_3 thin film on GaAs (001) substrate.[13] To further investigate the crystalline quality and orientations, the XRD experiments were conducted. Figure 1(e) displays sharp (003) family diffraction peaks in addition to the diffractive peaks from mica substrate, suggesting that the as-grown thin film exhibited a preferential alignment along *c*-axis.

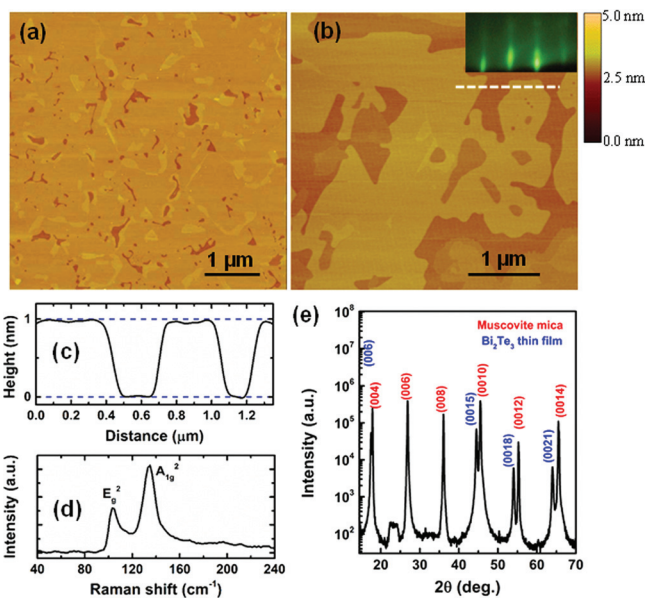

FIG. 1. AFM topographic images of (a) 4 QLs and (b) 10 QLs Bi_2Te_3 thin films on mica substrates. Inset in (b) shows a typical RHEED pattern for a 10 QLs Bi_2Te_3 thin film taken after the growth. (c) Profile along the dash line in (b), showing the height of Bi_2Te_3. (d) Raman spectrum measured from a 45 QLs Bi_2Te_3 thin film grown by MBE on a mica substrate. (e) XRD pattern of the sample in θ-θ geometry, indexed in blue for Bi_2Te_3 thin film and in red for muscovite mica substrate.

Systematic magnetoresistance (MR) measurements were performed to extract the phase coherence length in samples of varying thickness. Figure 2(a) shows the magnetoresistance as a function of magnetic field, defined as [R(B)-R(0)]/R(0). In the lower field regime ($-0.3\,T < B < +0.3\,T$), the thinner samples with a thickness of 4, 5, and 6 QLs show a sharp "dip" feature in the MR curves (inset of Fig. 2(a)), representing a characteristic feature of the WAL effect which originates from the conductance correction owing to the strong spin-orbit coupling in TIs.[14] Assuming that the inelastic scattering time (τ_ϕ) is much longer than the elastic and spin-orbit scattering time (τ_e and τ_{so}), the conductance correction, $\Delta G(B) = G(B) - G(0)$, can be well described by the Hikami-Larkin-Nagaoka (*HLN*) quantum interference theory[15]

$$\Delta G(B) = -\frac{\alpha e^2}{\pi h}\left[\Psi\left(\frac{1}{2}+\frac{h}{8e\pi L_\phi^2 B}\right) - \ln\left(\frac{h}{8e\pi L_\phi^2 B}\right)\right],$$

where α is the WAL coefficient which should be -0.5 for one topological surface accounting for the phase-coherent transport, L_ϕ is the phase coherence length, and $\Psi(x)$ is the digamma function. Notably, L_ϕ can be used as a criterion for the quality of TI thin films because it determines the phase-coherent transport.[4] Here, we exemplify a 5 QLs Bi_2Te_3 thin film to extract α and L_ϕ. Figure 2(b) displays the corresponding conductance correction plotted in the lower field regime

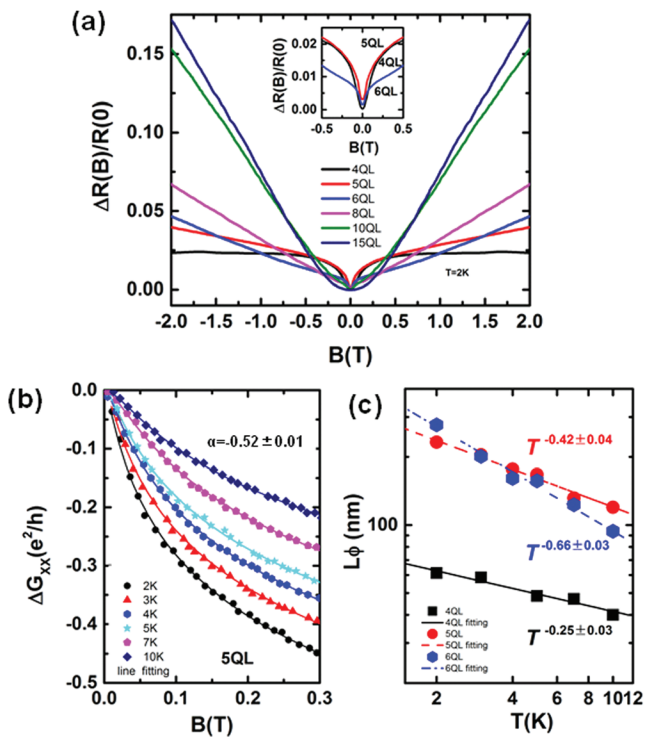

FIG. 2. (a) Normalized magnetoresistance data of Bi_2Te_3 thin films measured at 2 K. The inset highlights a deep cusp in MR data of 4, 5, and 6 QLs Bi_2Te_3 thin films in a relatively low field regime. (b) Conductance change of thinner samples in the low magnetic field regime with the *HLN* model fit. (d) Temperature dependence of the phase coherence length (L_ϕ) extracted from the *HLN* fit.

at different temperatures. By fitting to the *HLN* model, the data yield a coefficient of -0.52 ± 0.01 at all measured temperatures. Similarly, we acquired coefficients of -0.39 ± 0.04 and -0.40 ± 0.02 for the 4 QLs and 6 QLs Bi_2Te_3 thin films, respectively. All three coefficients are found close to -0.5, indicating that carrier transport is affected and governed by the strong spin-orbit interaction in the TI system.[16] The temperature dependence of the phase coherence length for three samples is shown in Fig. 2(c). The length monotonically increases as the decrease of the temperature, consistent with previous reports.[14,17] At 2 K, the 6 QLs thin film exhibits a phase coherence length of 277 nm, comparable to 331 nm obtained from 50 nm MBE-grown Bi_2Te_3 thin films on semi-insulating GaAs (111) substrate.[18] Temperature-dependent phase coherence lengths were further fitted by a power law ($L_\phi \sim T^\beta$) in which the β value was extracted as -0.25 ± 0.03, -0.42 ± 0.03, and -0.66 ± 0.04 for 4, 5, and 6 QLs thin films, respectively. Theoretically, β should be close to $-1/3$, $-1/2$, and $-3/4$ for 1D, 2D, and 3D systems.[18] Hence, the 5 and 6 QLs thin films behave like a 2D system. The 4 QLs thin film has a considerably low β value, which is presumably ascribed to the involvement of additional weakly temperature-dependent magnetic or nonmagnetic electron dephasing process.[19]

When a high magnetic field was applied, pronounced oscillations were observed in both R_{xx} and R_{yx}, enabling us to further probe the surface states and to evaluate the quality of the thin films. Figure 3(a) shows the Hall resistance R_{yx} of a 4 QLs Bi_2Te_3 thin film as a function of magnetic field at 2 K. The R_{yx} data display clear Shubnikov-de Hass (SdH) oscillations as shown in the lower inset with the first order derivative dR_{yx}/dB. The upper inset illustrates a fast Fourier transform (FFT) of the oscillations. Two well resolved frequencies $F_1 = 56$ T and $F_2 = 101$ T were identified. The nature of two-frequency SdH oscillations can presumably be attributed to the different carrier densities of the top and bottom surfaces.[4,20] In fact, the frequency is directly related to the size of the Fermi surface which can be quantitatively described by Onsager equation,[21] $F = (\hbar/(2\pi e))A$, where $\hbar$ is the reduced Planck's constant, e is the elementary electron charge, and A is the Fermi surface cross-section area (equal to πk_F^2). Assuming a circular 2D Fermi surface, the carrier density is determined by k_F via $n_{2D} = k_F^2/4\pi$.[22] Thus, two wave vectors, $k_{F1} = 4.1 \times 10^6\,\mathrm{cm}^{-1}$ and $k_{F2} = 5.5 \times 10^6\,\mathrm{cm}^{-1}$ can be deduced from the equations, which correspond to the 2D carrier density of surface electrons, $n_1 = 1.35 \times 10^{12}\,\mathrm{cm}^{-2}$ and $n_2 = 2.45 \times 10^{12}\,\mathrm{cm}^{-2}$, respectively. The Landau-level fan diagram for the oscillation in the dR_{yx}/dB is shown in Fig. 3(b), where the positions of minima in dR_{yx}/dB are plotted as a function of Landau index n. A linear fitting to this data gives an intercept of 0.65 ± 0.03, which deviates from the exact π-Berry phase. This could be due to the interference between the two frequencies as shown in the inset of Fig. 3(a).[6,23] Furthermore, we extract the cyclotron mass m_{cyc} by fitting the temperature dependence of the normalized oscillation amplitude with Lifshitz-Kosevich (LK) theory.[21] Figure 3(c) displays the normalized amplitude collected at 7.2 T. According to the LK equation, $\Delta\sigma_{xx}(T)/\Delta\sigma_{xx} = \lambda(T)/\sinh(\lambda(T))$, where the thermal factor $\lambda(T) = 2\pi^2 k_B T m_{cyc}/(\hbar e B)$ and k_B is the Boltzmann constant, we obtained cyclotron effective mass $m_{cyc} = 0.148 \pm 0.08\, m_e$ (m_e represents the free electron mass). Once m_{cyc} is known, the Fermi velocity can be calculated as $4.28 \pm 0.23 \times 10^5$ m/s with the equation $V_F = \hbar K_F/m_{cyc}$.[22] Then the Fermi level is estimated to be $E_F = m_{cyc} V_F^2 = 154 \pm 25$ meV above the Dirac point. Moreover, by applying the extracted m_{cyc}, the lifetime of the surface state, τ, can be deduced to be $(4.18 \pm 0.02) \times 10^{-13}$ s from the slope in the Dingle plot of $Ln[\Delta R_{xx} B \sinh(\lambda(T))] \sim [2\pi^2 E_F/(\tau e V_F^2)]$ (inset of Fig. 3(c)). The mean-free path, l, and the surface quantum mobility, μ_s, can be further calculated as $(1.79 \pm 0.02) \times 10^{-7}$ m and $0.48 \pm 0.03\ \mathrm{m^2\ V^{-1}\ s^{-1}}$, respectively. Remarkably, the surface mobility obtained here is comparable to that of the Bi_2Te_2Se thin films grown on BN substrates[24] and the Bi_2Te_3 single crystals,[22] again assuring the high quality of our thin films.

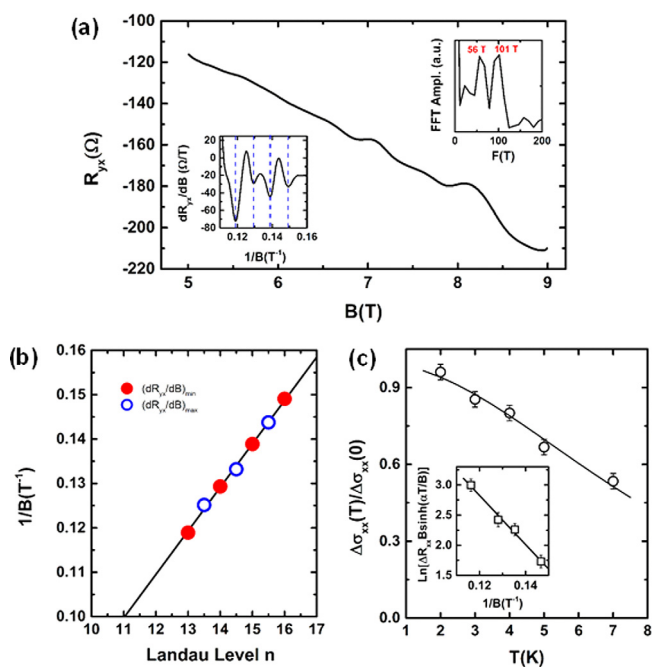

FIG. 3. SdH oscillations of a 4 QLs Bi_2Te_3 thin film. (a) Hall resistance R_{yx} plotted as a function of magnetic field at 2 K. The lower inset shows the first derivative of R_{yx} against 1/B. The upper inset shows the FFT of dR_{yx}/dB. (b) Landau level fan diagram for oscillation in dR_{yx}/dB. Maxima and minima in dR_{yx}/dB correspond to n and n + 1/2, respectively. (c) Temperature dependence of the SdH amplitudes of normalized conductivity.

To explore the potential optoelectronic applications, we have investigated the transmission spectra of the Bi_2Te_3 thin films on mica substrates as opposed to those of a bare mica wafer and an indium tin oxide (ITO) glass. As shown in Fig. 4, two sharp peaks observed at 1421 nm and 2194 nm in the spectrum of bare mica can be assigned to the OH and H_2O and Al-OH absorption feature, respectively.[25] In addition to these two peaks, the bare muscovite mica exhibits optical transparency in the measured wavelength range, permitting the evaluation of the absorption of the Bi_2Te_3 thin films. Although both the mica and the Bi_2Te_3 thin film have a nature of layered structure, the oscillations featured in the lower energy portion of the spectra can be mainly associated with the interference of the wave reflected in between the layers of mica, given the fact that the mica substrate is four orders of magnitude thicker than the Bi_2Te_3 thin films.[26,27]

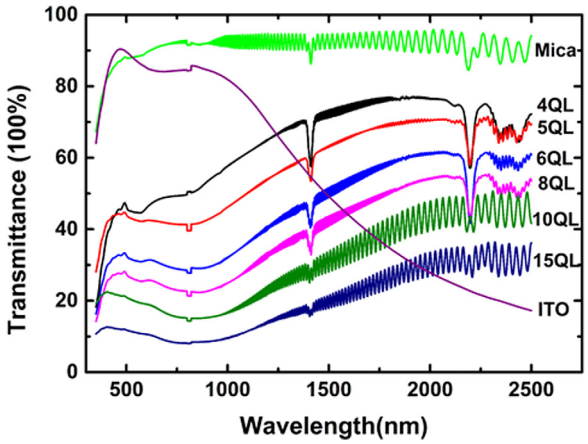

FIG. 4. UV-Vis-NIR spectra of Bi_2Te_3 thin films with different thicknesses on mica.

The absorption of Bi_2Te_3 thin films manifests evident thickness-dependent features in the entire wavelength range. Significantly, 4 QLs and 15 QLs Bi_2Te_3 thin films have an average visible transmittance of ~45% and ~10%, respectively, suggesting the high absorbance of the Bi_2Te_3 thin films. Moreover, similar to Bi_2Se_3 nanosheets on mica,[27] our ultrathin Bi_2Te_3 film exhibits a superior transmittance in range of 1200–2500 nm compared with ITO glass. These unique optical features of our Bi_2Te_3 thin films, together with the robust surface sates, provide a possibility to realize high-performance optoelectronics in specific spectrum ranges.

To summarize, high-quality Bi_2Te_3 thin films exhibiting atomically smooth terraces over several microns have been fabricated on insulating and flexible mica substrates by MBE. The relatively large phase coherence length of relatively thin samples extracted from the WAL effect, and the high mobility deduced by the quantum oscillations can be attributed to the reduced defect density epilayer grown by means of vdWE. The availability of such high quality TI thin films on the transparent mica substrates will facilitate the investigation of the quantum interference effect and the manipulation of the surface states, providing the possibility of exploring the potential application of TI in optoelectronics.

This work was supported by the National Young 1000 Talents Plan in China. N. Meyer and X. Y. Che would like to thank the financial support from the U.S. National Science Foundation under the Award No. 1201883.

[1]X. L. Qi and S. C. Zhang, Rev. Mod. Phys. **83**, 1057 (2011); J. E. Moore, Nature **464**, 194 (2010); O. V. Yazyev, J. E. Moore, and S. G. Louie, Phys. Rev. Lett. **105**, 266806 (2010); V. Goyal, D. Teweldebrhan, and A. A. Balandin, Appl. Phys. Lett. **97**, 133117 (2010).
[2]S. S. Hong, J. J. Cha, D. S. Kong, and Y. Cui, Nat. Commun. **3**, 757 (2012).
[3]H. D. Li, Z. Y. Wang, X. Kan, X. Guo, H. T. He, Z. Wang, J. N. Wang, T. L. Wong, N. Wang, and M. H. Xie, New J. Phys. **12**, 103038 (2010); M. L. Teague, H. Chu, F. X. Xiu, L. He, K. L. Wang, and N. C. Yeh, Solid State Commun. **152**, 747 (2012).
[4]A. A. Taskin, S. Sasaki, K. Segawa, and Y. Ando, Adv. Mater. **24**, 5581 (2012).
[5]S. Schreyeck, N. V. Tarakina, G. Karczewski, C. Schumacher, T. Borzenko, C. Brune, H. Buhmann, C. Gould, K. Brunner, and L. W. Molenkamp, Appl. Phys. Lett. **102**, 041914 (2013).
[6]Z. Ren, A. A. Taskin, S. Sasaki, K. Segawa, and Y. Ando, Phys. Rev. B **85**, 155301 (2012).
[7]A. Koma, Thin Solid Films **216**, 72 (1992).
[8]Y. S. Zhou, K. Wang, W. H. Han, S. C. Rai, Y. Zhang, Y. Ding, C. F. Pan, F. Zhang, W. L. Zhou, and Z. L. Wang, ACS Nano **6**, 6478 (2012); J. D. Grunwaldt, F. Atamny, U. Gobel, and A. Baiker, Appl. Surf. Sci. **99**, 353 (1996); M. I. B. Utama, F. J. Belarre, C. Magen, B. Peng, J. Arbiol, and Q. H. Xiong, Nano Lett. **12**, 2146 (2012).
[9]Y. Y. Li, G. A. Wang, X. G. Zhu, M. H. Liu, C. Ye, X. Chen, Y. Y. Wang, K. He, L. L. Wang, X. C. Ma, H. J. Zhang, X. Dai, Z. Fang, X. C. Xie, Y. Liu, X. L. Qi, J. F. Jia, S. C. Zhang, and Q. K. Xue, Adv. Mater. **22**, 4002 (2010).
[10]N. Bansal, Y. S. Kim, M. Brahlek, E. Edrey, and S. Oh, Phys. Rev. Lett. **109**, 116804 (2012).
[11]X. X. Yu, L. He, M. R. Lang, W. J. Jiang, F. X. Xiu, Z. M. Liao, Y. Wang, X. F. Kou, P. Zhang, J. S. Tang, G. Huang, J. Zou, and K. L. Wang, Nanotechnology **24**, 015705 (2013).
[12]Y. Liu, M. Weinert, and L. Li, Phys. Rev. Lett. **108**, 115501 (2012); M. X. Wang, C. H. Liu, J. P. Xu, F. Yang, L. Miao, M. Y. Yao, C. L. Gao, C. Y. Shen, X. C. Ma, X. Chen, Z. A. Xu, Y. Liu, S. C. Zhang, D. Qian, J. F. Jia, and Q. K. Xue, Science **336**, 52 (2012).
[13]V. Russo, A. Bailini, M. Zamboni, M. Passoni, C. Conti, C. S. Casari, A. L. Bassi, and C. E. Bottani, J. Raman Spectrosc. **39**, 205 (2008); H. L. Cao, R. Venkatasubramanian, C. Liu, J. Pierce, H. R. Yang, M. Z. Hasan, Y. Wu, and Y. P. Chen, Appl. Phys. Lett. **101**, 162104 (2012); X. Liu, D. J. Smith, J. Fan, Y. H. Zhang, H. Cao, Y. P. Chen, J. Leiner, B. J. Kirby, M. Dobrowolska, and J. K. Furdyna, *ibid.* **99**, 171903 (2011).
[14]S. Matsuo, T. Koyama, K. Shimamura, T. Arakawa, Y. Nishihara, D. Chiba, K. Kobayashi, T. Ono, C. Z. Chang, K. He, X. C. Ma, and Q. K. Xue, Phys. Rev. B **85**, 075440 (2012).
[15]S. Hikami, A. I. Larkin, and Y. Nagaoka, Prog. Theor. Phys. **63**, 707 (1980).
[16]H. Steinberg, J. B. Laloë, V. Fatemi, J. S. Moodera, and P. Jarillo-Herrero, Phys. Rev. B **84**, 233101 (2011).
[17]L. H. Bao, L. He, N. Meyer, X. F. Kou, P. Zhang, Z. G. Chen, A. V. Fedorov, J. Zou, T. M. Riedemann, T. A. Lograsso, K. L. Wang, G. Tuttle, and F. X. Xiu, Sci. Rep. **2**, 726 (2012).
[18]H. T. He, G. Wang, T. Zhang, I. K. Sou, G. K. L. Wong, J. N. Wang, H. Z. Lu, S. Q. Shen, and F. C. Zhang, Phys. Rev. Lett. **106**, 166805 (2011).
[19]S. P. Chiu and J. J. Lin, Phys. Rev. B **87**, 035122 (2013).
[20]A. A. Taskin, S. Sasaki, K. Segawa, and Y. Ando, Phys. Rev. Lett. **109**, 066803 (2012).
[21]D. Shoenberg, *Magnetic Oscillations in Metals* (Cambridge University Press, 1984).
[22]D. X. Qu, Y. S. Hor, J. Xiong, R. J. Cava, and N. P. Ong, Science **329**, 821 (2010).
[23]L. Fang, Y. Jia, D. J. Miller, M. L. Latimer, Z. L. Xiao, U. Welp, G. W. Crabtree, and W. K. Kwok, Nano Lett. **12**, 6164 (2012).
[24]P. Gehring, B. F. Gao, M. Burghard, and K. Kern, Nano Lett. **12**, 5137 (2012).
[25]W. Herrmann, M. Blake, M. Doyle, D. Huston, J. Kamprad, N. Merry, and S. Pontual, Econ. Geol. **96**, 939 (2001).
[26]M. I. B. Utama, Z. P. Peng, R. Chen, B. Peng, X. L. Xu, Y. J. Dong, L. M. Wong, S. J. Wang, H. D. Sun, and Q. H. Xiong, Nano Lett. **11**, 3051 (2011).
[27]H. L. Peng, W. H. Dang, J. Cao, Y. L. Chen, W. Wu, W. S. Zheng, H. Li, Z. X. Shen, and Z. F. Liu, Nat. Chem. **4**, 281 (2012).